MEASUREMENT OF THE REACTION $e^+e^- \rightarrow \nu\bar{\nu}\gamma$ AT LEP

G. RAVEN*
NIKHEF, Kruislaan 409, 1098 SJ Amsterdam, The Netherlands

ABSTRACT

The measurement of final states consisting of a single photon and missing energy in e^+e^- collisions around the Z pole, based on an integrated luminosity of 57.3 pb^{-1}, collected with the L3 detector during 1990–1993 is presented. The number of light neutrino generations is determined ($N_\nu = 3.01 \pm 0.09 \pm 0.08$), and limits on both the magnetic moment of ν_τ ($\mu_{\nu_\tau} < 4.1 \cdot 10^{-6}\ \mu_B$ at 90% CL) and the coupling of the Z to the photon are set.

1 Introduction

The fermions in the Standard Model are grouped together in families. With the recent discovery of the top quark by the CDF and D0 collaborations[1], all members of the first three families, with the exception of the ν_τ, have been observed. The question arises whether there are families beyond these three.

Before the startup of LEP and SLC, four measurements addressed this question, all using the fact that each family contains a distinct neutrino :

- The Kamiokande and IMB measurements[2] of the $\bar{\nu}_e$ flux produced by supernova SN1987A:
$$N_\nu = 2.5^{+4.1}_{-0.8} \text{ or } N_\nu < 8 \text{ at } 90\% \text{ CL}.$$
- The measurement[3] of the relative abundance of ^{4}He in the universe:
$$N_\nu = 2.3 \pm 0.8 \text{ or } N_\nu < 3.6 \text{ at } 95\% \text{ CL}.$$
- The determination of the total Z width from $p\bar{p}$ collider experiments[4]:
$$N_\nu < 4.8 \text{ at } 90\% \text{ CL}.$$
- The upper limit on the cross section of $e^+e^- \rightarrow \nu\bar{\nu}\gamma$ from the measurements[5] at PEP, PETRA and TRISTAN:
$$N_\nu < 3.9 \text{ at } 90\% \text{ CL}.$$

---

*Representing the L3 Collaboration.

2 The determination of N_ν from the Z lineshape

From the measurements of the cross sections for $\mathrm{e^+e^-} \to$ *hadrons* and $\mathrm{e^+e^-} \to$ *leptons* at center of mass energies around to the Z resonance at LEP and SLC , one can extract the invisible width of the Z as the difference between the total width and the sum of the hadronic and leptonic widths:

$$\Gamma_{\mathrm{inv}} = \Gamma_{\mathrm{Z}} - \Gamma_{\mathrm{had}} - 3\Gamma_\ell .$$

An additional generation of (light) neutrinos increases Γ_{Z} by $\approx 6\%$. In order to reduce correlations between the fitted parameters, a four parameter fit (assuming lepton universality) to the measured cross sections is performed, using $m_{\mathrm{Z}}, \Gamma_{\mathrm{Z}}, \sigma_0^{\mathrm{had}}$ and R_{had}, where

$$\sigma_0^{\mathrm{had}} = \frac{12\pi\Gamma_e\Gamma_{\mathrm{had}}}{m_{\mathrm{Z}}^2\Gamma_{\mathrm{Z}}^2} \ , \ R_{\mathrm{had}} = \frac{\Gamma_{\mathrm{had}}}{\Gamma_\ell}.$$

To minimize the m_{top} and m_{Higgs} dependence, one then uses

$$N_\nu = \frac{\Gamma_{\mathrm{inv}}}{\Gamma_\ell}\left(\frac{\Gamma_\ell}{\Gamma_\nu}\right)_{\mathrm{SM}} = \left(\sqrt{\frac{12\pi R_{\mathrm{had}}}{m_{\mathrm{Z}}^2\sigma_0^{\mathrm{had}}}} - R_{\mathrm{had}} - 3\right)\left(\frac{\Gamma_\ell}{\Gamma_\nu}\right)_{\mathrm{SM}}$$

to extract the number of neutrino generations. The L3 result[6], from the data collected during 1990–1993, is:

$$N_\nu = 2.98 \pm 0.03.$$

3 The measurement of N_ν from the reaction $\mathrm{e^+e^-} \to \nu\bar{\nu}\gamma$

A complementary method to determine N_ν is the measurement of the the cross section of the reaction $\mathrm{e^+e^-} \to \gamma+$*missing energy* which, in the Standard Model, is dominated by the decay of the Z into neutrino pairs, with a small contribution arising from the t-channel W exchange diagrams (Figure 1).

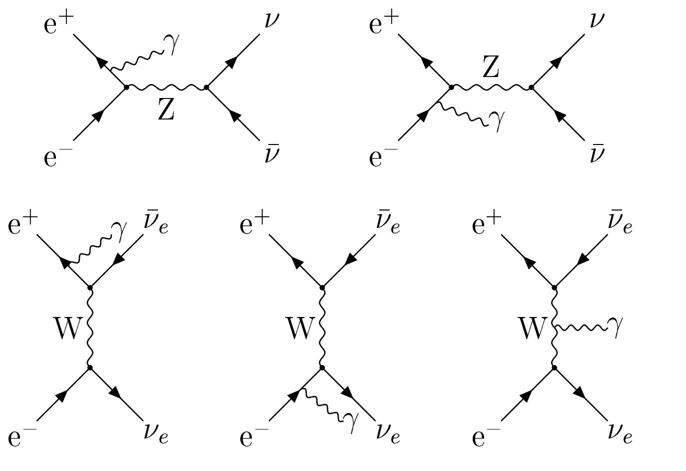

Figure 1: Lowest order Feynman diagrams for the process $\mathrm{e^+e^-} \to \nu\bar{\nu}\gamma$.

One can write the differential cross section for this process as

$$\frac{d^2\sigma}{dE_\gamma\ d\cos\theta_\gamma} = H(E_\gamma, \cos\theta_\gamma, s)\ \sigma_0(s') \tag{1}$$

where the radiator function $H(E_\gamma, \cos\theta_\gamma, s)$ describes the probability of radiating a photon of energy E_γ under an angle θ_γ with respect to the beam axis, $\sqrt{s}$ is the center of mass energy, and $\sigma_0(s')$ the cross section for the process $e^+e^- \to \nu\bar{\nu}$ at the reduced center of mass energy $s' = s(1 - 2E_\gamma/\sqrt{s})$. In the improved Born approximation[7], $\sigma_0(s)$ is given by:

$$\sigma_0(s) = \frac{12\pi}{m_Z^2}\ \frac{sN_\nu\Gamma_\nu\Gamma_e}{(s - m_Z^2)^2 + s^2\Gamma_Z^2/m_Z^2} + \mathrm{W\ contribution.} \tag{2}$$

The W contribution to the cross section varies as a function of the center of mass energy, and, for the energies accessed sofar in the LEP energy scans, it is less than 4%.

As can be seen from Eq. 2, if one fixes Γ_Z to the value determined from the Z lineshape, the cross section depends linearly on N_ν, and an additional generation of neutrinos increases the cross section by $\approx 30\%$. Because H is a rapidly decreasing function of the photon energy, the measurement benefits from the ability to measure and trigger on photons of low energy. It also implies that the maximum sensitivity to N_ν is not reached at $\sqrt{s} = m_Z$, but at center of mass energies slightly above the Z resonance, depending on the minimal required photon energy.

3.1 The L3 detector

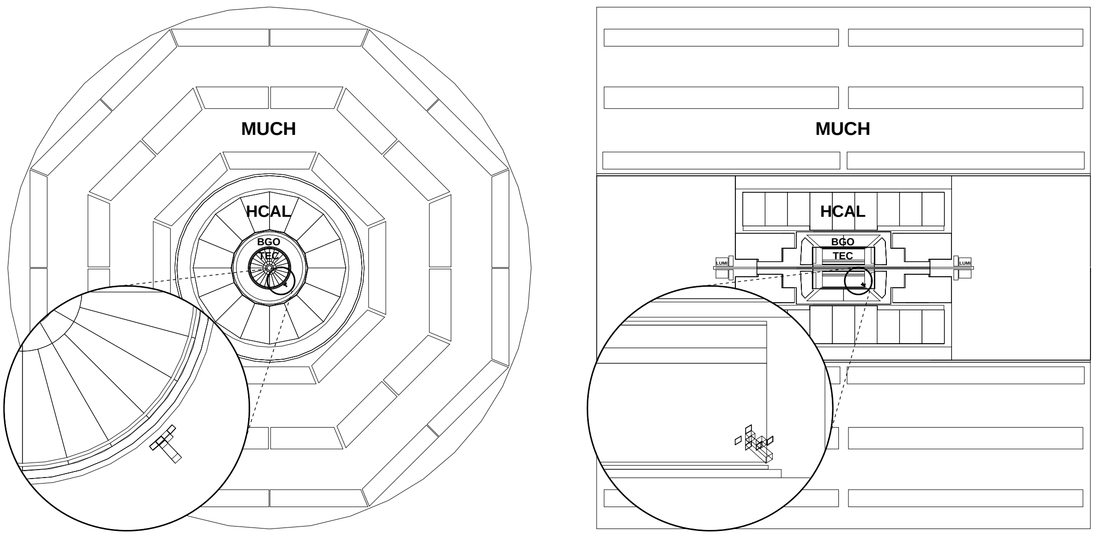

(a) $r - \phi$ view (b) $r - z$ view

Figure 2: An event display of a single photon candidate in the L3 detector. Except for a single 1.58 GeV cluster in the BGO calorimeter no activity is detected.

The L3 detector at LEP covers 99% of the full solid angle and is designed to measure the energy and position of leptons and photons with high precision. A detailed description of the detector can be found elsewhere[8], only the features relevant to the single photon analysis are described here.

The detector consists of a central tracking chamber (TEC), a high resolution electromagnetic calorimeter consisting of 10734 bismuth germanium oxide (BGO) crystals, a hadron calorimeter (HCAL) and a muon spectrometer (MUCH). Between the BGO and the HCAL a cylindrical array of 30 scintillation counters is installed. All sub-detectors are installed inside a magnetic field of 0.5 T along the beam axis, which is provided by a solenoidal magnet with an inner diameter of 12 m.

An example of a single photon candidate can be seen in Figure 2. Since the only visible signal is the presence of a single cluster in the BGO calorimeter, processes where final state particles escape detection can fake this signature. This is illustrated in Figure 3 in the case of the dominant background, low q^2 radiative Bhabha scattering. If both electrons escape at small enough angles with respect to the beam axis these events are indistinguishable from the signal. This background can be reduced by requiring that the observed photon has sufficient transverse momentum, such that at least one of the electrons should scatter more than an angle θ_{veto}, the smallest angle at which particles can be detected. In the case of L3, $\theta_{\mathrm{veto}} = 1.5^\circ$ as defined by the luminosity monitors (LUMI).

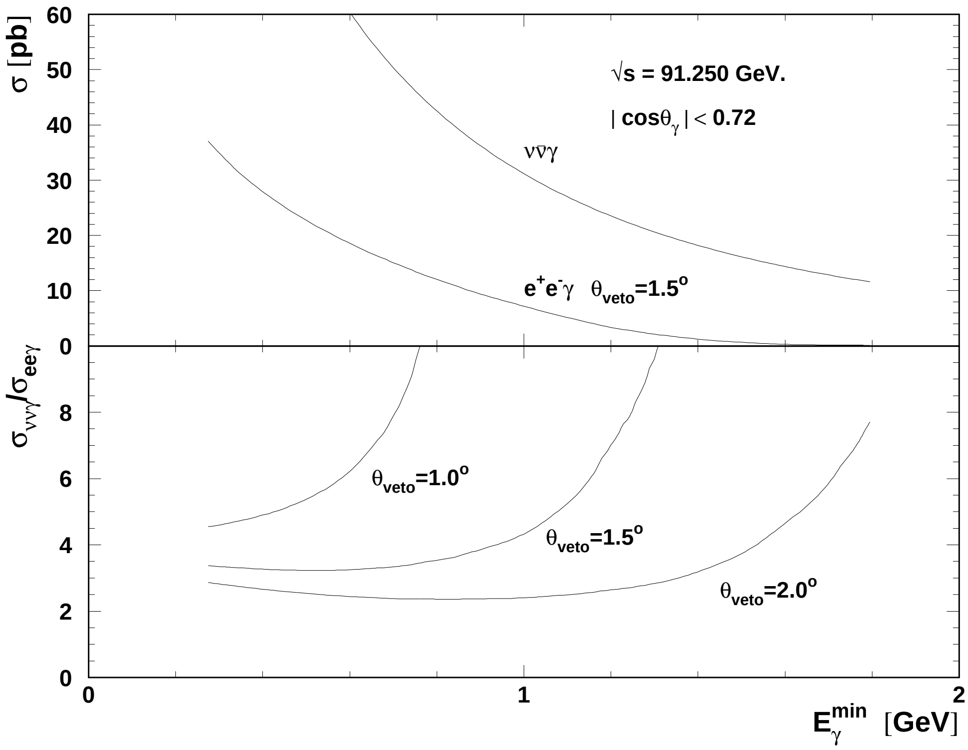

Figure 3: Signal and background cross sections and their ratios as function of the minimum required photon energy, for different values of θ_{veto}, the smallest angle at which particles can be detected.

3.2 Event Selection

The selection of single photon candidates requires:

- a reconstructed photon in the electromagnetic calorimeter with an energy larger than 1 GeV, at a polar angle between 44° and 136°.
- no other activity in the detector:
  - no charged tracks;
  - no additional clusters reconstructed in the electromagnetic calorimeter;
  - no significant amount of energy deposited in either of the luminosity monitors;
  - no reconstructed muon;
  - no energy deposited in the hadron calorimeter beyond what is expected from noise.

As mentioned before, the main background consists of $\mathrm{e^+e^-} \to \mathrm{e^+e^-}\gamma$. Less important sources of backgrounds include $\mathrm{e^+e^-} \to \gamma\gamma\gamma$, $\mathrm{e^+e^-} \to \mu^+\mu^-\gamma$, $\mathrm{e^+e^-} \to \tau^+\tau^-\gamma$ and the production of resonances through photon-photon interactions, $\mathrm{e^+e^-} \to \mathrm{e^+e^-X}$, where X is *e.g.* a $\pi^0, \eta, \eta', a_2, f_2$. Another source of background is cosmic rays.

In addition, detector occupancy effects can lead to the misidentification of a fraction of the genuine single photon events, causing them to be rejected. The probability for this has been determined from unbiased events which are triggered at random beam crossings.

The preliminary results of the event selection for '92 and '93, combined with our published[9] results from '90 and '91 are summarized in table 1.

Table 1: Luminosity, observed and expected number of events.

	$\sqrt{s}$(GeV)	$\int \mathcal{L}dt(\mathrm{pb}^{-1})$	N_{obs}	$N^{\nu\bar{\nu}\gamma}_{\mathrm{expected}}$	$N^{\mathrm{background}}_{\mathrm{expected}}$
1990	88.3–94.3	2.98	61	49.4	8.8
1991	88.6–93.7	9.57	202	196.6	29.9
1992	91.294	19.13	399	315.0	66.9
1993	89.452	5.32	46	30.7	20.5
	91.211	12.38	247	208.3	45.7
	93.034	7.90	371	364.7	28.0

The selection efficiency is determined from events, generated with the NNGSTR Monte Carlo generator[10], simulated using the L3 detector simulation package based on GEANT3[11], and corrected for the measured detector occupancy effects. The trigger efficiency is determined both from a measurement, based on a sample of isolated electrons which are triggered by a dedicated trigger, and from a simulation, which incorporates the measured gain and resolution of each trigger channel.

The knowledge of the absolute energy scale and energy resolution of the electromagnetic calorimeter is checked by reconstructing the invariant masses of π^0's and η's in hadronic Z decays[12].

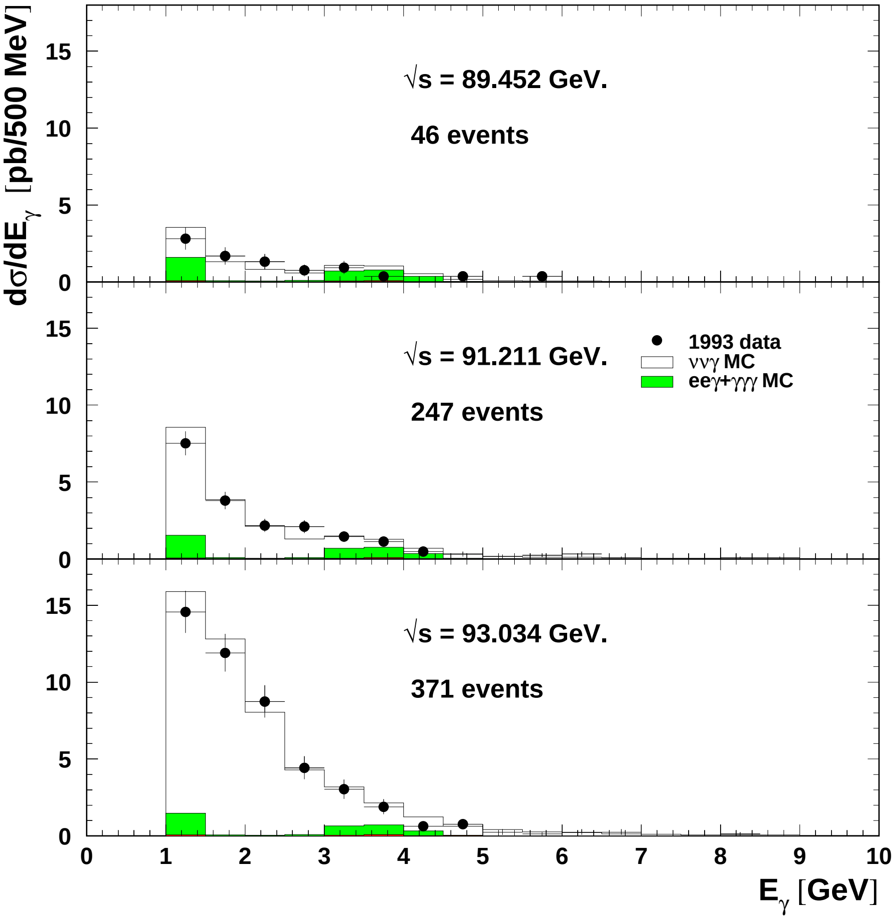

Figure 4: Measured spectra for the '93 data sample at three different center of mass energies. The increase in background around 3–4 GeV is due to a small detection gap around a three degrees angle to the beam axis.

The number of light neutrino generations is determined from a binned likelihood fit to the differential cross section as a function of energy at the various $\sqrt{s}$ points. The number of expected events per bin is calculated from Eq. 1, where the radiator function H is taken from a calculation by Nicrosini and Trentadue[13], which takes into account the full $\mathcal{O}(\alpha^2)$ matrix element and which resummes the leading soft photon contributions to all orders.

The L3 lineshape measurement[14] is used to constrain m_Z and Γ_Z. The value of $\sin^2\theta_W^{\rm eff}$ from the same measurement is used to obtain the value of Γ_e. The result of the fit is shown in Figure 5. Combining the preliminary result from the fit to the 1992 and 1993 data, $N_\nu = 2.99 \pm 0.10 \pm 0.08$, with our published 1990 and 1991 results[9], one finds:

$$\boxed{N_\nu = 3.01 \pm 0.09 \pm 0.08.}$$

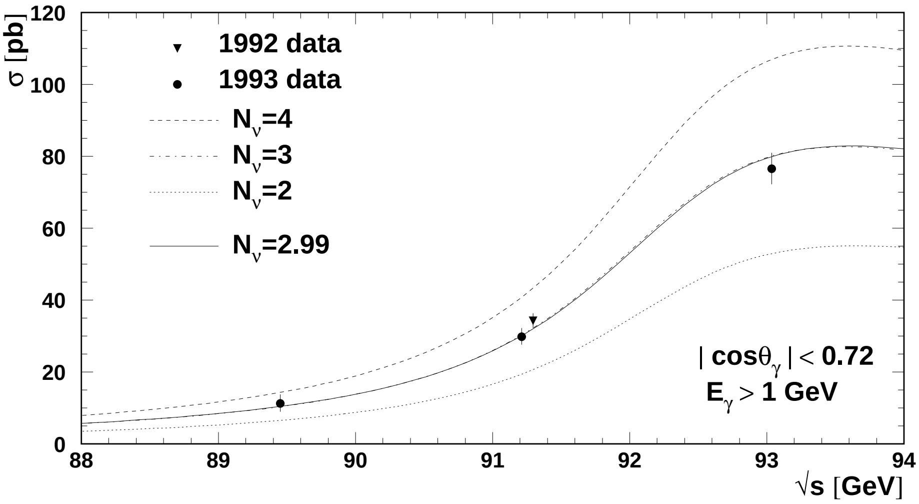

Figure 5: Comparison of the single photon cross section and the predictions for two, three and four generations, and the result of the likelihood fit to the 1992 and 1993 data, $N_\nu = 2.99$.

4 Searches for physics beyond the Standard Model

4.1 Magnetic moment of ν_τ

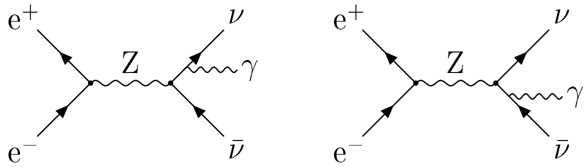

Figure 6: The diagrams most sensitive to μ_ν at center of mass energies close to the Z resonance

Events with a single photon signature can also be produced by radiation of a photon from the final state (anti) neutrino produced in Z decays if this (anti) neutrino has a non-zero magnetic moment (see Figure 6). Assuming that the contribution to the production of photons due to the magnetic moment does not interfere appreciably with the contribution from initial state radiation, the production cross section of photons beyond what is expected from initial state radiation is proportional to the square of the magnetic moment.

In case of ν_e and ν_μ, very strict limits exist from measurements of $\nu - e$ scattering[15]:

$$\begin{aligned} \mu_{\nu_e} &< 10.8 \cdot 10^{-10}\ \mu_B \text{ at } 90\% \text{ CL}, \\ \mu_{\nu_\mu} &< 7.4 \cdot 10^{-10}\ \mu_B \text{ at } 90\% \text{ CL}. \end{aligned}$$

Therefore only a limit on the magnetic moment of the ν_τ is considered.

To obtain an upper-limit, the number of events expected as function of μ_{ν_τ} is calculated, using the differential Born cross section[16], taking into account the center of mass energy, the geometric acceptance of the selection cuts, the combined trigger and selection efficiency and initial-state radiation. The upper limit on the excess events

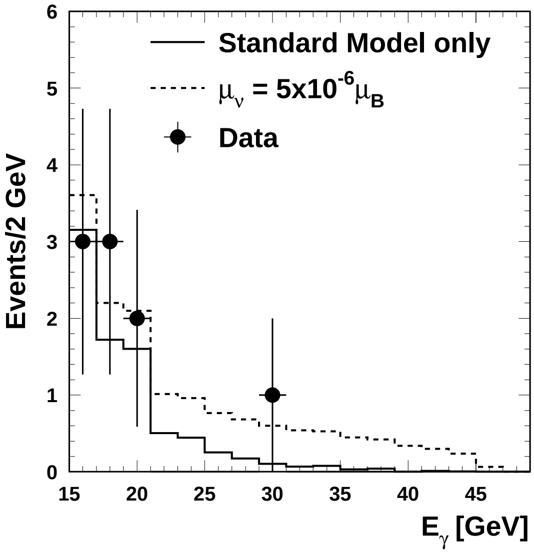

Figure 7: Measured spectrum of single photon events and the prediction for $\mu_\nu = 5 \cdot 10^{-6} \mu_{\mathrm{B}}$.

allowed by the data is determined from Poisson statistics from the observed number of events with an energy greater than half the beam energy and the expected Standard Model background. Using this procedure the following upperlimit is obtained[17]:

$$\boxed{\mu_{\nu_\tau} < 4.1 \cdot 10^{-6}\ \mu_B \text{ at } 90\% \text{ CL.}}$$

The above bound applies to both static and transition magnetic moments. It is competitive with the bound of $4 \cdot 10^{-6}\ \mu_B$ (90% CL) from low-energy experiments[18] and the determination of the invisible Z width from the lineshape measurement, which yields a limit of $3.8 \cdot 10^{-6}\ \mu_B$ (90% CL). With respect to these bounds, the limit obtained here is unique in being a direct limit of the magnetic moment at $q^2 = 0$.

4.2 Limits on ZZγ couplings

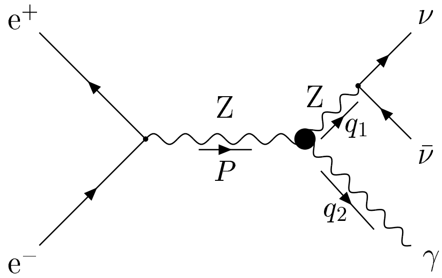

Figure 8: The ZZγ vertex.

Single photon events are also sensitive to coupling between the Z boson and the photon. The most general vertex, which is both Lorentz and gauge invariant, can be parametrized in terms of four independent dimensionless form factors[19] h_i^{Z}, $i =$

1, 2, 3, 4:

$$\Gamma^{\alpha\beta\mu}_{Z\gamma Z}(q_1, q_2, P) = \frac{P^2 - q_1^2}{m_Z^2} \times \left(h_1^Z \, (q_2^\mu g^{\alpha\beta} - q_2^\alpha g^{\mu\beta}) + h_2^Z \, \frac{P^\alpha \left((P \cdot q_2) g^{\mu\beta} - q_2^\mu P^\beta \right)}{m_Z^2} + \right.$$
$$\left. h_3^Z \, \varepsilon^{\mu\alpha\beta\rho} q_{2\rho} + h_4^Z \, \frac{P^\alpha \varepsilon^{\mu\beta\rho\sigma} P_\rho q_{2\sigma}}{m_Z^2} \right).$$

The contributions proportional to h_1^Z and h_2^Z are CP-violating, whereas the other two are CP-conserving. Although at tree level all four terms are zero, at one loop level the two CP conserving terms become non-zero, but too small to lead to an observable deviation from zero (*e.g.* $h_3^Z = \mathcal{O}(10^{-4})$). Thus any observation of a non-zero coupling constant h_i^Z would indicate physics beyond the Standard Model. Figure 9 shows the sensitivity of the energy spectrum of single-photon events to a non-zero value of h_3^Z.

In order to set limits on the form factors h_i^Z, the following parameterization is adopted[19]:

$$h_i^Z = \frac{h_{i0}^Z}{(1 + P^2/\Lambda_Z^2)^{n_i}},$$

where P is the momentum of the initial-state Z, and Λ_Z a scale parameter.

Unitarity requires $n_1, n_3 > 1.5$ and $n_2, n_4 > 2.5$. For this analysis $n_1 = n_3 = 3.0$ and $n_2 = n_4 = 4.0$ is used. With this choice of exponents the terms proportional to h_{10}^Z and h_{30}^Z have the same high energy behaviour as those proportional to h_{20}^Z and h_{40}^Z

To obtain upper limits on h_{i0}^Z, events were generated for various combinations of the coupling constants and passed through the detector simulation and analysis programs. The results were used to obtain the number of events expected for the various values of h_{i0}^Z and Λ_Z. Given that the LEP center of mass energy is small compared to the chosen scale Λ_Z, there is not much variation as the scale Λ_Z is increased from 0.5 TeV to 1.0 TeV. The unitarity limit is very sensitive to Λ_Z, decreasing as Λ_Z^{-3} along the h_{30}^Z axis and as Λ_Z^{-4} along the h_{40}^Z axis, for our choice of n_i.

The 95% CL contours from the L3 measurement[17] in the $h_{10}^Z(h_{30}^Z) - h_{20}^Z(h_{40}^Z)$ plane are shown in Figure 9 for scales $\Lambda_Z = 0.5$ TeV and $\Lambda_Z = 1.0$ TeV. Also plotted in this figure is the CDF result from their measurement[20] of the reaction $p\bar{p} \to l^+l^-\gamma X$, for an assumed scale of 0.5 TeV. The CDF contour appears rotated with respect to the L3 contour, as the contribution to the amplitude of terms proportional to $h_4^Z(h_2^Z)$ rises steeply with respect to those from the terms involving $h_3^Z(h_1^Z)$ as the (effective) center of mass energy increases from m_Z to the range of several hundred GeV at the Tevatron.

5 Conclusions

Using our measurement of the reaction $e^+e^- \to \gamma +$ *missing energy*, the number of light neutrino generations is determined to be $N_\nu = 3.01 \pm 0.09 \pm 0.08$, in good

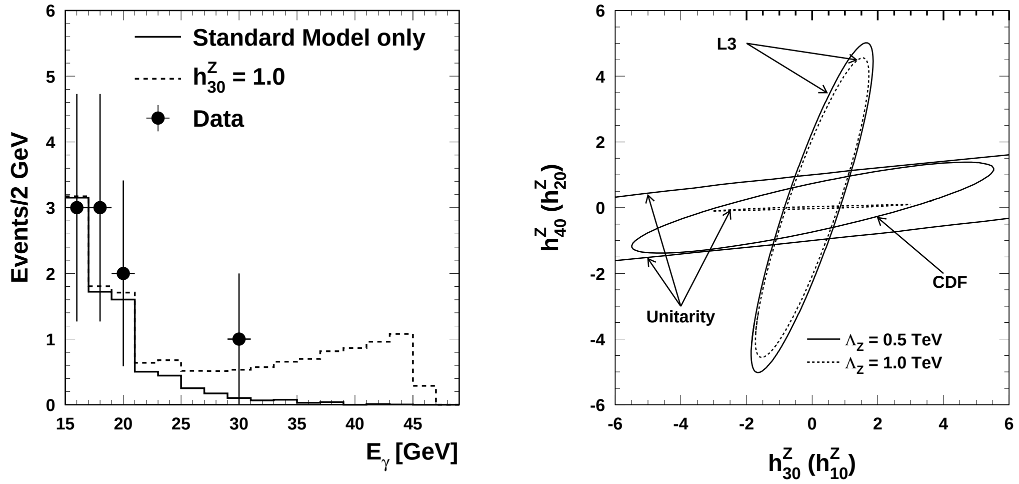

(a) (b)

Figure 9: The photon spectrum as expected for $h^Z_{30} = 1$ (a) and the upper limits (95% CL) on the Zγ coupling from the L3 single photon data for two different values of Λ_Z (b).

agreement with the result from the Z lineshape measurements. Using the high energy part of the photon spectrum, limits have been set on the magnetic moment of ν_τ, $\mu_{\nu_\tau} < 4.1 \cdot 10^{-6}\ \mu_B$ at 90% CL, and the coupling between the Z boson and the photon.

References

1. CDF collaboration, F. Abe *et al.*, FERMILAB-PUB-95/022-E;
   D0 collaboration, S. Abachi *et al.*, FERMILAB-PUB-95/028-E.
2. Kamiokande II Collaboration, K. Hirata *et al.*, *Phys. Rev. Lett.* **58**, 1490 (1987);
   IMB III Collaboration, R. M. Bionta *et al.*, *Phys. Rev. Lett.* **58**, 1494 (1987);
   J. Ellis and K. Olive, *Phys. Lett.* **B193**, 525 (1987);
   D. Schramm, *Comm. Nucl. Part. Phys.* **A17**, 239 (1987).
3. G. Steigman, D. N. Schramm, J. E. Gunn, *Phys. Lett.* **B66**, 202 (1977).
4. R. Ansari *et al.*, *Phys. Lett.* **B186**, 440 (1987);
   C. Albajar *et al.*, *Phys. Lett.* **B198**, 271 (1987).
5. C. Hearty *et al.*, *Phys. Rev.* **D39**, 3207 (1989);
   H. J. Behrend *et al.*, *Phys. Lett.* **B215**, 186 (1988);
   W. T. Ford *et al.*, *Phys. Rev.* **D33**, 3472 (1986);
   K. Abe *et al.*, *Phys. Lett.* **B232**, 431 (1989).
6. The LEP collaborations, ALEPH, DELPHI, L3, OPAL and the LEP Electroweak Working Group, CERN-PPE/94-187.

7. M. Consoli *et al.*, in *Z physics at LEP 1*, ed. G. Altarelli *et al.*, CERN 89-08 Vol. 1, 7 (1989).
8. L3 Collaboration, B. Adeva *et al.*, *Nucl. Instrum. Methods* **A289**, 35 (1990).
9. L3 Collaboration, B. Adeva *et al.*, *Phys. Lett.* **B275**, 209 (1992);
   L3 Collaboration, O. Adriani *et al.*, *Phys. Lett.* **B292**, 463 (1992).
10. F. A. Berends *et al.*, *Nucl. Phys.* **B301**, 583 (1988).
11. R. Brun *et al.*, *GEANT3 Users Guide*, CERN/DD/EE/84.1.
12. L3 Collaboration, M. Acciarri *et al.*, *Phys. Lett.* **B328**, 223 (1994).
13. O. Nicrosini and L. Trentadue, *Nucl. Phys.* **B318**, 1 (1989).
14. L3 Collaboration, M. Acciarri *et al.*, *Z. Phys.* **C62**, 223 (1994).
15. D. A. Krakauer *et al.*, *Phys. Lett.* **B252**, 177 (1990).
16. T. M. Gould and I. Z. Rothstein, *Phys. Lett.* **B333**, 545 (1994).
17. L3 Collaboration, M. Acciarri *et al.*, CERN-PPE/94-216.
18. H. Grotch and R. W. Robinett, *Z. Phys.* **C39**, 553 (1988).
19. U. Baur and E. L. Berger, *Phys. Rev.* **D47**, 4889 (1993).
20. CDF Collaboration, F. Abe *et al.*, FERMILAB-PUB-94/304-E.